Table VI. Orbital Parameters Used in the Extended Hückel Calculations

atom	orbital	VOIE, eV	exponent
Al	3s	-12.3	1.167
	3p	-6.5	1.167
Al	3s	-12.3	**1.383**
	3p	-6.5	**1.383**
Mg	3s	-9.0	0.950
	3p	-4.5	0.950
Mg	3s	-9.0	**1.167**
	3p	-4.5	**1.167**
O	2s	-32.3	2.275
	2p	-14.8	2.275
Si	3s	-17.3	1.383
	3p	-9.2	1.383
H	1s	-13.6	1.300

Table VII. First Brillouin Zone Symmetry Points and Lines[a]

layer-group symmetry	$\mathbf{k}_\Gamma$	$\mathbf{k}_K$	$\mathbf{k}_M$	$\mathbf{k}_{\Delta(\Gamma K)}$	$\mathbf{k}_{\Sigma(\Gamma M)}$	$\mathbf{k}_{T(MK)}$
p6mm	*6mm*	*3m*	*2mm*	*m*	*m*	*m*
p3m1	*3m*	1	*m*	1	*m*	1

[a] Reciprocal space basis vectors: $\mathbf{g}_1 = (2\pi/a\sqrt{3}, -2\pi/a)$ and $\mathbf{g}_2 = (4\pi/a\sqrt{3}, 0)$. $\mathbf{k}_\Gamma = [0, 0]$; $\mathbf{k}_K = [^2/_3, ^1/_3]$; $\mathbf{k}_M = [^1/_2, 0]$; $\mathbf{k}_{\Delta(\Gamma K)} = [2\alpha, \alpha]$, $0 < \alpha < ^1/_3$; $\mathbf{k}_{\Sigma(\Gamma M)} = [\beta, 0]$, $0 < \beta < ^1/_2$; $\mathbf{k}_{T(MK)} = [^1/_2 + \gamma, 2\gamma]$, $0 < \gamma < ^1/_6$.

populations of the nearest-neighbor and, to a much lesser extent, next-nearest-neighbor atoms will increase. The opposite effects will occur if the substituting atom is more electronegative (e.g., phosphorus). Excess negative charge deposited on the framework when the substituting atom has a lower nuclear charge than silicon will be partitioned between the site of the substituting atom and its nearest-neighbor oxygens. The perturbation will largely be restricted to the TO_4Si_x ($x = 3$ or 4) unit because nearest-neighbor orbital interactions are so strong.

Technically, the octahedral sites in phyllosilicates are extra-framework sites. Coulombic interactions between the substituting atom and oxygens in the octahedral sheet can dominate orbital interactions without jeopardizing the structure of phyllosilicates. Orbital interactions between magnesium and oxygen are negligible. When magnesium replaces aluminum in the octahedral sheet of dioctahedral montmorillonites or celadonite, next-nearest-neighbor magnesium-aluminum interactions represent the only means of displacing electron density away from the substitution site. The excess negative charge displaced from the substitution site bypasses nearest-neighbor oxygens and is deposited on next-nearest-neighbor aluminum. Shifts in the Al Kβ transition in response to aluminum substitution by magnesium are taken as evidence that next-nearest-neighbor interactions are possible. A decrease in the binding energy of photoelectrons ejected from aluminum in a magnesium-rich celadonite would provide a further test of the hypothesis that most of the displaced charge resides on the next-nearest-neighbor aluminum atoms.

Acknowledgment. R.H. is grateful to the National Science Foundation for its support of this work through Research Grant CHE 8406119. W.B. is grateful to the Cornell Chapter of Sigma Xi for its early support of this study under its Grants-in-Aid Program.

Appendix

The orbital parameters used in our extended Hückel, tight-binding calculations appear in Table VI. The important distances used in our calculations are d(Si-O) = 1.618 Å,[4] $d(Al_{tet}-O)$ = 1.748 Å,[4] $d(Al_{oct}-O)$ = 1.924 Å (mean $d(Al_{oct}-O)$[48]), d(Mg-O) = 2.067 Å (mean d(Mg-O)[49]), d(O-H) = 0.971 Å (d(H-O)[48]), $d(O-O)_{Mg}$ (shared-edge) = 2.430 Å, and $d(O-O)_{Al}$ (shared-edge) = 2.567 Å. The 4-fold oxygen polyhedra coordinating silicon or aluminum have point symmetry $\bar{4}3m$, while coordination polyhedra for both magnesium and aluminum have point symmetry $3m$. The octahedral sheet has layer-group symmetries $c2/m$ in pyrophyllite and $c121$ in celadonite. The $^2_\infty[Si_2O_5^{2-}]$, tetrahedral sheet has layer-group symmetry $p3m1$ pyrophyllite and celadonite.

A set of 24 k-points for the *p6mm* layer group, a set of 44 k-points for the *p3m1* layer group, and a set of 16 k-points for the $c121$ and $c2/m$ layer groups were used in the irreducible wedges of the first Brillouin zones.[50] Density-of-state and COOP calculations, which require integration over the first Brillouin zone, were based on these special k-point sets. Since Cunningham did not include a k-point set for the trigonal lattice in his paper, we generated the k-point set for *p3m1* by taking an irreducible wedge double that of *p6mm* and using symmetry to generate the extra points in this new wedge from the smaller *p6mm* set.

Registry No. Al, 7429-90-5; Mg, 7439-95-4.

(48) Lee, J. H.; Guggenheim, S. *Am. Mineral.* **1981**, *66*, 350.
(49) Mellini, M. *Am. Mineral.* **1982**, *67*, 587.
(50) Cunningham, S. L. *Phys. Rev. B: Solid State* **1974**, *10*, 4988.

Contribution from the Materials and Chemical Sciences Division, Lawrence Berkeley Laboratory, Berkeley, California 94720, Laboratoire de Radiochimie, Institut de Physique Nucleaire, Universite de Paris-Sud, B. P. 1, 91406 Orsay Cedex, France, Department of Physics, Kalamazoo College, Kalamazoo, Michigan 49007, and Chemistry Division B.220, AERE Harwell, Oxfordshire OX11 0RA, England

Analysis of the $5f^1 \rightarrow 6d^1$ Transitions in PaX_6^{2-} (X = Cl, Br) and $Pa^{4+}/ThBr_4$

N. Edelstein,*,† J. C. Krupa,‡ R. C. Naik,‡,§ K. Rajnak,⊥ B. Whittaker,∥ and D. Brown∥

Received March 23, 1988

The optical spectra of $Pa^{4+}/ThBr_4$ and M_2PaX_6 (M = Cs, X = Cl; M = NEt_4, X = Cl, Br) in the visible and ultraviolet ranges have been obtained and are analyzed in terms of a Hamiltonian including the crystal field and spin-orbit interactions for the 6d configuration. A lower limit of ~13 800 cm^{-1} is obtained for the total crystal field splitting of PaX_6^{2-}. Spin-orbit coupling constants of ζ_{6d} = 2050 cm^{-1} (PaX_6^{2-}) and ζ_{6d} = 1570 cm^{-1} ($Pa^{4+}/ThBr_4$) are obtained. Relative shifts of 5f-6d configuration centroids in crystals are compared to the free-ion values.

Introduction

The $5f^1$ configuration is an attractive system to study because of the simplicity of its electronic spectrum. For the ion Pa^{4+}, relatively few data have been reported. Axe was the first to report and analyze intraconfigurational f → f transitions in the system Pa^{4+}/Cs_2ZrCl_6.[1] This work was followed by optical studies on other Pa^{4+} hexahalo compounds[2,3] and on Pa^{4+} diluted in single

† Lawrence Berkeley Laboratory.
‡ Universite de Paris-Sud.
§ Permanent address: Spectroscopy Division, Bhabha Atomic Research Center, Trombay, Bombay-400085, India.
⊥ Kalamazoo College.
∥ AERE Harwell.

(1) Axe, J. D. Ph.D. Thesis, University of California, Berkeley, CA, 1980; UCRL-9293.
(2) Brown, D.; Whittaker, B.; Edelstein, N. *Inorg. Chem.* **1974**, *13*, 1805.
(3) Brown, D.; Whittaker, B.; Edelstein, N. *Inorg. Chem.* **1976**, *15*, 511.

0020-1669/88/1327-3186$01.50/0

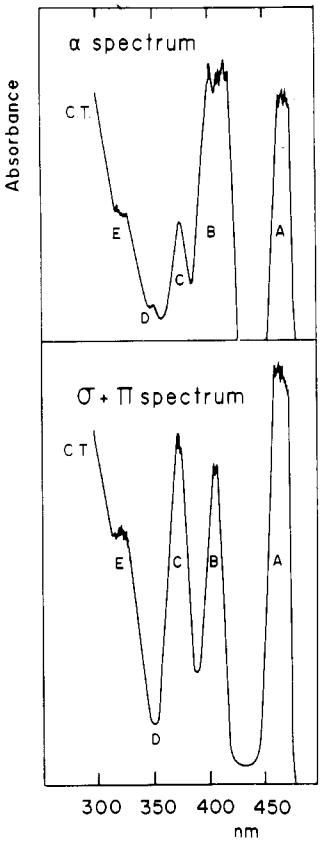

Figure 1. Optical spectra of $Pa^{4+}/ThBr_4$ at 77 K: (top) α spectrum; (bottom) unpolarized spectrum. C.T. is the charge-transfer band.

crystals of $ThBr_4$ and $ThCl_4$.[4]

Strong absorption bands in the visible range were first observed by Axe in Pa^{4+}/Cs_2ZrCl_6 but were not conclusively assigned.[1] Recently, Naik and Krupa have reported absorption and fluorescence spectra in $Pa^{4+}/ThBr_4$ that have been assigned to transitions between the ground $5f^1$ and the excited $6d^1$ configurations.[5] We report herein more detailed absorption and fluorescence spectra of $Pa^{4+}/ThBr_4$ and solution absorption spectra of M_2PaX_6 (M = Cs, X = Cl; M = NEt_4, X = Cl, Br). The observed bands are assigned and the data analyzed in terms of a Hamiltonian containing spin–orbit and crystal field interactions.

Experimental Section

Absorption spectra of $Pa^{4+}/ThBr_4$ were obtained at 300 and 77 K in the visible and ultraviolet ranges with a Cary 17 spectrophotometer, with a Spex Model 1403 spectrophotometer using a tungsten lamp as a source, and photographically with a Jarrell-Ash F-6 spectrograph. For the absorption studies, the $Pa^{4+}/ThBr_4$ crystal was oriented such that the $\vec{c}$ axis was either parallel to the direction of propagation of the light (α spectrum, which corresponds to σ polarization) or perpendicular to this direction ($\sigma + \pi$ spectrum) (see Figure 1). Conventional polarized σ and π spectra were also obtained with the $\vec{c}$ axis perpendicular to the direction of the propagation of light by use of polarizing filters. No differences in the fluorescence spectra were observed with conventional polarization measurements. The dependence on excitation frequency was obtained in the fluorescence spectra by pumping into the different absorption bands (Figure 2). Various argon ion laser lines, a N_2-pumped dye laser, and the filtered 2537-Å Hg line were used for excitation. Solution spectra (under an atmosphere of Ar) of Cs_2PaCl_6, $(NEt_4)_2PaCl_6$, and $(NEt_4)_2PaBr_6$ dissolved in CH_3CN were obtained at room temperature on a Cary 14 spectrophotometer. A solution spectrum of $(Et_4N)_2PaBr_6$ is shown in Figure 3.

(4) Krupa, J. C.; Hubert, S.; Foyentin, M.; Gamp, E.; Edelstein, N. *J. Chem. Phys.* **1983**, *78*, 2175.
(5) Naik, R. C.; Krupa, J. C. *J. Lumin.* **1984**, *31/32*, 222.

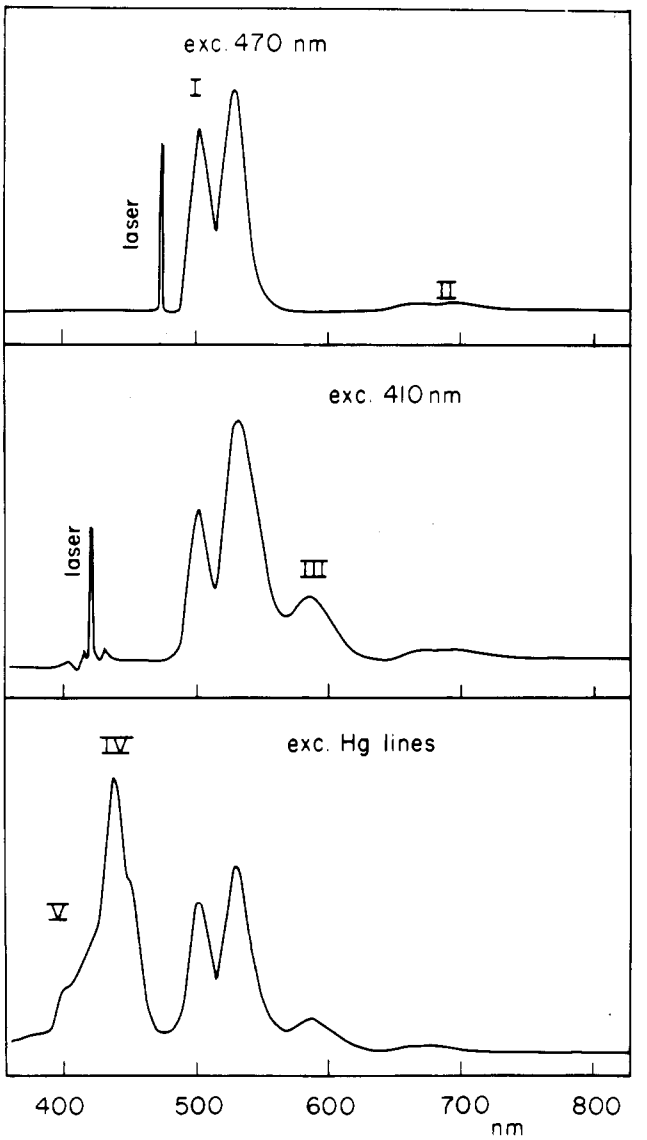

Figure 2. Fluorescence spectra with various excitation frequencies.

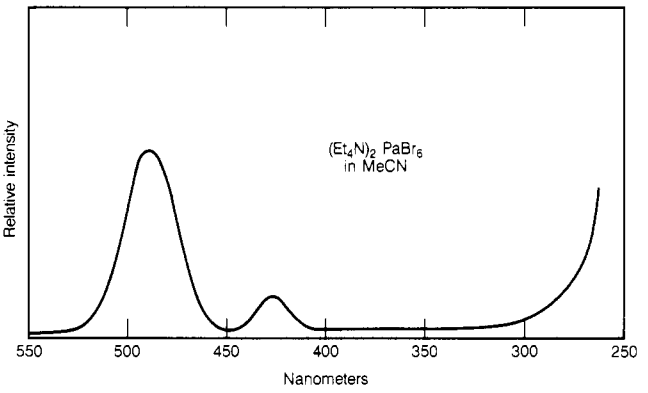

Figure 3. Room-temperature optical spectrum of $(NEt_4)_2PaBr_6$ in CH_3CN solution.

Theory and Assignments

The Hamiltonian for a one-electron configuration outside a closed shell may be written as the sum of three terms

$$H = H_{so} + H_{CF} + E_{av}$$

where

$$H_{so} = \zeta_{nl}\vec{l}\cdot\vec{s} \qquad nl = 5f, 6d$$

and for D_{2d} symmetry

$$H_{CF} = B_0^2C_0^2 + B_0^4C_0^4 + B_4^4[C_{-4}^4 + C_4^4] + B_0^6C_0^6 + B_4^6[C_{-4}^6 + C_4^6]$$

E_{av} is defined as the center of gravity of the $5f^1$ or $6d^1$ configuration. Sixth-order terms in H_{CF} occur only for the f^1 configuration. In the case of O_h symmetry, $B_0^2 = 0$, $B_4^4 = (5/14)^{1/2}B_0^4$, and $B_4^6 = -(7/2)^{1/2}B_0^6$.

A number of absorption bands were observed for $Pa^{4+}/ThBr_4$ in the wavelength range of 5000–3000 Å (see Figure 1). The three highest energy bands were measured as shoulders on the broad background of the charge-transfer transition observed in pure $ThBr_4$. Since only five f → d transitions are allowed, the highest energy band was assigned to a charge-transfer transition in $Pa^{4+}/ThBr_4$.

The ground state for the $5f^1$ configuration of $Pa^{4+}/ThBr_4$ is of Γ_6 symmetry. In accord with the electric dipole selection rules for D_{2d} symmetry ($\Gamma_6 \leftrightarrow \Gamma_7$ ($\vec{E} \parallel \vec{c}$) π polarization; Γ_6 or $\Gamma_7 \leftrightarrow \Gamma_6$ or Γ_7 ($\vec{E} \perp \vec{c}$) σ polarization) bands that appeared to be relatively less intense in the α spectra (which corresponds to σ polarization) than in the σ and π spectra were assigned to the Γ_6 excited states. These assignments are shown in Table I. Conventional polarized absorption spectra showed no extinctions, only relative intensity changes in the bands similar to those shown in Figure 1 (α spectrum similar to σ spectrum; π spectrum similar to π plus σ spectrum).

The spin–orbit and crystal field parameters obtained by fitting the calculated energies to the experimental values are given in Table II. Because there are four parameters (besides E_{av}, the center of gravity of the configuration) and four energy differences, the calculated and experimental energies agree. Calculated relative intensities, based on the wave functons obtained from these assignments, are also given in Table I.

Fluorescence bands from the 6d levels to the ground $5f^1$ states of $Pa^{4+}/ThBr_4$ were obtained by selective excitation into the various 6d absorption bands. Excitation at any wavelength into the lowest energy 6d band (A in Figure 1) gave rise to two pairs of emission bands, I and II as shown in Figure 2. These emission bands are assigned as transitions from the lowest 6d crystal field level to the two spin–orbit-split multiplets $^2F_{5/2}$ (I) and $^2F_{7/2}$ (II) as shown in Figure 4. Selective excitation in the second absorption band (B in Figure 1) resulted in the addition of a new feature (III in Figure 2), which was assigned to transitions from the B level to the $^2F_{7/2}$ multiplet (Figure 4). When Hg emission lines were used for excitation, the new fluorescent bands IV and V appeared and were assigned as transitions from the B and C levels to the ground $^2F_{5/2}$ multiplet.

For the octahedral anion PaX_6^{2-}, the crystal field splits the $6d^1$ configuration into a t_{2g} lower state and a higher e_g state. Spin–orbit coupling will split the lower t_{2g} state into a Γ_6 and a Γ_8 state with the splitting $\sim{}^3/_2\zeta_d$, where ζ_d is the 6d spin–orbit coupling constant. From the spectrum (and similar spectra for the other PaX_6^{2-} complexes) shown in Figure 3, we obtain $\zeta_d \approx 2000$ cm^{-1}. The e_g state is obscured in the ultraviolet region by a broad continuum at ~3000 Å. There is some indication of a level just before this broad band, which we have tentatively assigned to the $5f^1(\Gamma_6) \rightarrow 5d^1ne_g$) transitions (see Table III). With this assignment the parameters given in Table IV were obtained. This assignment represents a lower limit to the crystal field splitting. Again the experimental and calculated energies agree because of the equal number of levels and energy differences. Calculated relative intensities are given in Table III.

Discussion

The $5f^1$ and $6d^1$ parameters (Table V) for octahedral PaX_6^{2-} have the same signs. In a point-charge model (which is known to be incorrect but is used here qualitatively), the cubic parameter B_0^4 scales as the ratio $\langle r^4\rangle_{6d}/\langle r^4\rangle_{5f}$. Values of the energies of the $5f^1$ and $6d^1$ configurations, spin–orbit coupling constants, and various radial averages calculated from the Cowan HF code with a relativistic correction (HFR)[6] are given in Table V. The experimental data do not follow these ratios. The spin–orbit coupling constant for the $6d^1$ configuration is ~0.6 of the calculated free-ion value.

(6) Cowan, R. D. *The Theory of Atomic Structure and Spectra*; University of California Press: Berkeley, CA, 1981; p 214.

Table I. $Pa^{4+}/ThBr_4$ Energy Levels for the $6d^1$ Configuration

		calcd rel intens		
assgnt	energy, cm^{-1}	σ polarizn	π polarizn	unpolarized
Γ_7	20710	0.2	1.0	0.6
Γ_6	23600	1.18	0	0.59
Γ_7	26310	0.122	0.124	0.123
Γ_6	28160	0.24	0	0.12
Γ_7	30110	0.19	0.82	0.51

Table II. Parameter Values (cm^{-1}) for $Pa^{4+}/ThBr_4$

	$5f^1$	$6d^1$		$5f^1$	$6d^1$
E_{av}	3496	25778	B_0^6	−1162	...
ζ	1533	1567	B_4^4	−1990	−10430
B_0^2	−1047	1629	B_4^6	623	...
B_0^4	1366	3038	$N_v/(4\pi)^{1/2}$	1212.5	

Table III. PaX_6^{2-} Assignments from CH_3CN Solutions

	energy, cm^{-1}			calcd rel intens
assgnt	Cs_2PaCl_6	$(NEt_4)_2PaCl_6$	$(NEt_4)_2PaBr_6$	(unpolarized)
Γ_8	20780	20860	19280	1
Γ_6	24340	24550	22770	0.1
Γ_8'	32780[a]	33350[a]	33180[a]	0.6

[a] Tentative assignment.

Table IV. Parameter Values (cm^{-1}) for PaX_6^{2-} (X = Cl, Br)

	Cs_2PaCl_6		$(NEt_2)_4PaCl_6$		$(NEt_2)_4PaBr_6$	
	$5f^1$	$6d^1$	$5f^1$	$6d^1$	$5f^1$	$6d^1$
E_{av}	4245	26289	4441	26591	4237	25539
ζ	1490	2021	1523	2092	1535	2023
B_0^4	7104	20831	6665	21720	5413	25146
B_0^6	670	...	394	...	−68	...
$N_v/(4\pi)^{1/2}$	3145		2925		2363	

Table V. HFR Values for Pa^{4+} Free Ion

	E_{av}, cm^{-1}	ζ_{nl}, cm^{-1}	$\langle r^2\rangle$, au	$\langle r^4\rangle$, au	$\langle r^6\rangle$, au
$5f^1$	0	1834	2.222	9.025	61.10
$6d^1$	45075	3095	6.209	56.33	705.6

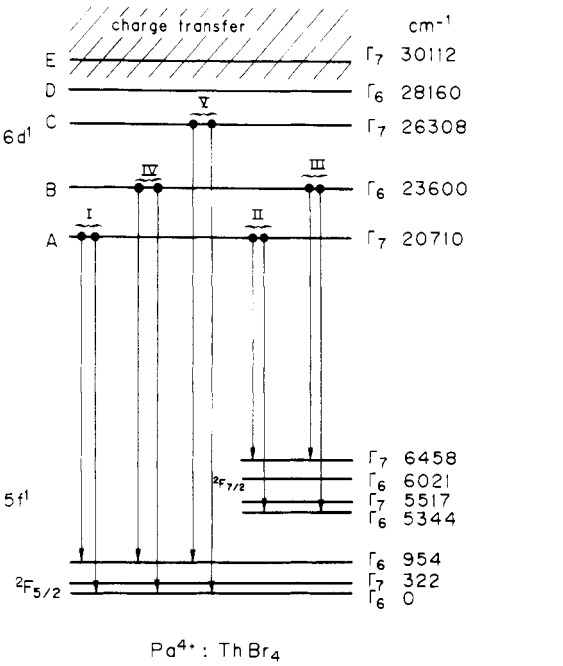

Figure 4. Assignments of the fluorescence bands obtained by selective excitation.

For the tetragonal crystal $ThBr_4$, the sign of B_0^2 for the $6d^1$ configuration is opposite that of the $5f^1$ configuration and $B_0^4(6d^1)$ is less than three times the value for $B_0^4(5f^1)$. However $B_4^4(6d^1)$ is ~5 times greater. Interestingly, the signs and relative magnitudes of the crystal field parameters for $Pa^{4+}/ThBr_4$ ($6d^1$) are similar to those found for $Ce^{3+}/LuPO_4$ ($5d^1$), which also has D_{2d} symmetry at the metal ion site.[7] The signs of the crystal field parameters for $Pa^{4+}/ThBr_4$ ($5f^1$) are the same as found for $Ce^{3+}/LuPO_4$ ($4f^1$) except for B_0^2, which is large and negative for Pa^{4+} and is very small and positive for Ce^{3+}.[4,7]

The total crystal field splitting of the $6d^1$ configuration for the octahedral anion $PaCl_6^{2-}$ is on the order of 13 800 cm^{-1}. This value seems rather low when compared with the reported weak d–d bands of the six-coordinate $NbCl_6^{2-}$ ($4d^1$) and $TaCl_6^{2-}$ ($5d^1$) of ~20 000 cm^{-1}[8] and the lower limit found for $CeCl_6^{3-}$ of 15 000 cm^{-1}.[9] Because of the uncertainty in the assignment of the highest energy band in PaX_6^{2-} (X = Cl, Br), and the expectation that the total crystal field splitting for a $6d^1$ configuration should be greater than for a $4d^1$ or $5d^1$ configuration with the same ligand and geometry, it is best to regard the value of ~13 800 cm^{-1} as a lower limit. Nevertheless, the spin–orbit coupling constant $\zeta_{6d} \approx 2050$ cm^{-1} compared to the free-ion calculation of ~3000 cm^{-1} suggests that covalent effects are quite important in the $6d^1$ configuration.

In $Pa^{4+}/ThBr_4$, $\zeta_{6d} \approx 1570$ cm^{-1}, an even lower value than found for the $PaBr_6^{2-}$ ion. In addition, the total crystal field splitting is only about ~10 000 cm^{-1}. In octahedral symmetry the Pa–Br bond length is shorter than found in $Pa^{4+}/ThBr_4$, which should result in a stronger crystal field. The Pa^{4+} ion in a D_{2d} site may be considered to be at the center of two tetrahedra, with the tetrahedron with the shortest bond distance giving the larger contribution to the crystal field. However, this contribution (in a point-charge model) would be only four-ninths of that of octahedral coordination at the same bond distance. Thus, the smaller crystal field splitting for the $6d^1$ configuration in D_{2d} symmetry than in octahedral symmetry is qualitatively consistent with the point-charge model.

The Auzel parameter, $N_v/(4\pi)^{1/2}$, can be used as a measure of the crystal field strength for f^n ions. The values for the $5f^1$ configuration are given in Tables II and IV for PaX_6^{2-} and $Pa^{4+}/ThBr_4$. By this measure, the $5f^1$ crystal field strength is greater for Pa^{4+} in octahedral symmetry than for Pa^{4+} in dodecahedral symmetry, which again qualitatively agrees with the results for the $6d^1$ configuration.

Data are available for the $4f^1 \rightarrow 5d^1$ transitions of Ce^{3+} diluted in $LuPO_4$.[7] This ion is also at a site of D_{2d} symmetry. The total $5d^1$ crystal field splitting is on the order of ~20 000 cm^{-1}, and the spin–orbit coupling constant is approximately the same as the free-ion value, $\zeta_{5d} \approx 1000$ cm^{-1}. Since the crystal field splitting for a 6d configuration should be greater than for a 5d configuration in the same host, these data suggest the $LuPO_4$ host has a considerably larger crystal field than $ThBr_4$.

From the HFR calculations shown in Table V, the difference in the centers of gravity (E_{av}) between the $5f^1$ and $6d^1$ configurations is ~45 000 cm^{-1}. Fitting the free-ion data for the isoelectronic series Ra^+, Ac^{2+}, Th^{3+}, and U^{5+} gives a value of approximately 50 000 cm^{-1} for the Pa^{4+} free ion.[10-12] Tables II and IV show this difference to be ~22 000 cm^{-1} for the Pa^{4+} complexes. This difference in the corresponding configruations in $Ce^{3+}/LuPO_4$ ($5d^1$ and $4f^1$) is ~40 000 cm^{-1}.[7] For the Ce^{3+} free ion, this energy difference is 49 943 cm^{-1}[13] while the HFR calculations give 45 366 cm^{-1}. Thus, the 6d–5f energy difference is much more strongly affected by the crystal field than the corresponding 5d–4f energy difference.

In the crystal field model, the energy difference between the centers of gravity of configurations is determined by the differences in the spherically symmetric terms (i.e., $B_0^0(6d) - B_0^0(5f)$ for Pa^{4+}; $B_0^0(5d) - B_0^0(4f)$ for Ce^{3+}) of the crystal field Hamiltonians. The various interactions that contribute to these parameters have recently been discussed.[14]

Conclusion

Crystal field analyses of the spectra of the $6d^1$ configuration of $Pa^{4+}/ThBr_4$ and PaX_6^{2-} (X = Cl, Br) have shown that both the crystal field and spin–orit coupling parameters are much smaller than might have been expected by extrapolation from Ce^{3+} or consideration of ions such as $NbCl_6^{2-}$ and $TaCl_6^{2-}$. The differences in the total crystal field splittings for Pa^{4+} in the two different crystal symmetries agree qualitatively with a point-charge model. The difference between the centers of gravity of the $6d^1$ and $5f^1$ configurations decreases markedly for Pa^{4+} in the crystal when compared to that for the free ion. Such a dramatic effect is not found for the differences of the centers of gravity between the $5d^1$ and $4f^1$ configurations for $Ce^{3+}/LuPO_4$ and Ce^{3+} free ion.

Acknowledgment. This work was supported in part by the Director, Office of Energy Research, Office of Basic Energy Sciences, Chemical Sciences Division, U.S. Department of Energy, under Contract No. DE-AC03-76SF00098.

(7) Williams, G.; Edelstein, N., unpublished work.
(8) Lever, A. B. P. *Inorganic Electronic Spectroscopy*, 2nd ed.; Elsevier: Amsterdam, 1984; p 392.
(9) Reisfeld, R.; Jørgensen, C. K. *Lasers and Excited States of Rare Earths*; Springer-Verlag: Berlin, FRG, 1977; p 37.
(10) Klinkenberg, P. F. A.; Lang, R. J. *Physica (Amsterdam)* **1949**, *15*, 774.
(11) Moore, C. E. *Atomic Energy Levels*; National Bureau of Standards: Washington, DC, 1958; Vol. III.
(12) Kaufman, V.; Radziemski, L. J., Jr. *J. Opt. Soc. Am.* **1976**, *66*, 599.
(13) Martin, W. C.; Zalubas, R.; Hagan, L. "*Atomic Energy Levels-The Rare Earth Elements*"; Report No. NSRDS-NBS60; National Bureau of Standards: Washington, DC, 1978.
(14) Aull, B. F.; Jenssen, H. P. *Phys. Rev. B: Condens. Matter* **1986**, *34*, 6640.